Space-shifting digital holography with dc term removal

Yanchao Dong and Jian Wu*

School of Physics and Nuclear Energy Engineering, Beijing University of Aeronautics and Astronautics, 37 Xueyuan Road, Beijing 100191, China

**Corresponding author: jwu2@buaa.edu.cn*

Received January 21, 2010; revised March 5, 2010; accepted March 12, 2010; posted March 17, 2010 (Doc. ID 123126); published April 15, 2010

We describe a numerical space-shifting reconstruction approach in digital holography. This method is able to remove the dc term in the reconstruction very effectively by utilizing the periodicity and the space-shifting property of inverse discrete Fourier transform. Since the entire process does not need any additional holograms and specific requirements to recording optics, this approach can be a really convenient, practical, and widely effective way to remove the dc term from in-line or off-axis digital holography. © 2010 Optical Society of America

OCIS codes: 090.1995, 100.3010, 070.2025.

In digital holography, people have been searching for an effective and practical approach to removing a dc term or zero-order diffractive image from the hologram reconstruction to acquire clear reconstructed images. This is particularly necessary to the in-line digital holography, as in which the reconstructed image at the center is fully superposed with the zero-order image. So far, a number of techniques on eliminating the zero-order diffraction have been reported [1–15]. However, most of them cannot be really an effective way to eliminate the zero-order image under the in-line circumstance. Although the methods based on the phase-shifting technique are able to resolve this problem effectively for both in-line and off-axis circumstances [2–5], some specific optical requirements in recording holograms, e.g., the use of multiple holograms and phase elements, make it hard to use these techniques in practical environments due to the complex of multiple hologram acquisition and processing as well as the sensitivity of phase variation to the environment.

Thus, here we describe what we believe to be a novel numerical space-shifting reconstruction approach, with which the dc term in the reconstruction can be removed very effectively, even if the image is fully superposed with the zero-order diffraction. The entire process is convenient in manipulation due to the purely numerical processing without any additional requirements to the recording optics.

In digital holography, the hologram recorded with a CCD can be characterized mathematically by [16]

$$
\begin{aligned}
h_{\mathrm{CCD}}(\xi,\eta) &= \frac{1}{4\Delta\xi\Delta\eta} h(\xi,\eta)\left[\mathrm{rect}\left(\frac{\xi}{\Delta\xi}\right)\mathrm{rect}\left(\frac{\eta}{\Delta\eta}\right)\right.\\
&\quad \left.\otimes\,\mathrm{comb}\left(\frac{\xi}{2\Delta\xi}\right)\mathrm{comb}\left(\frac{\eta}{2\Delta\eta}\right)\right]\\
&\quad \times \mathrm{rect}\left(\frac{\xi}{M\Delta\xi}\right)\mathrm{rect}\left(\frac{\eta}{N\Delta\eta}\right),\\
&= A(\xi,\eta)\cdot h(\xi,\eta),
\end{aligned}
\tag{1}
$$

where (ξ,η) is the hologram plane. $h(\xi,\eta)$ is the hologram function generated by coherent superposition of both object and reference waves. $\mathrm{rect}(\cdot)$ and $\mathrm{comb}(\cdot)$ are the rectangle and the Dirac comb functions, respectively. The symbol $\otimes$ denotes the convolution operator. M and N are the horizontal and vertical pixel numbers of the CCD, respectively. The corresponding pixel sizes are $\Delta\xi$ and $\Delta\eta$, $\xi = k\Delta\xi$, $\eta = l\Delta\eta$, $k=0,1,2,3\ldots M-1$, $l=0,1,2,3\ldots N-1$. $2\Delta\xi$ and $2\Delta\eta$ in the Dirac combs in Eq. (1) determine the sampling frequencies for the hologram fringes.

With the Fresnel transformation of the hologram reconstruction, the discrete complex amplitude, $\Gamma(m,n)$ of the reconstruction wave-field can be obtained by inverse discrete Fourier transform (IDFT) of $R(k,l)h_{CCD}(k,l)\exp[-j\pi/(\lambda d)(k^2\Delta\xi^2 + l^2\Delta\eta^2)]$ [1]. The result can be finally expressed as

$$
\begin{aligned}
\Gamma(m,n) &= IDFT\{A(k,l)\cdot U(k,l)\}\\
&= IDFT\{A(k,l)\}\otimes IDFT\{U(k,l)\}.
\end{aligned}
\tag{2}
$$

$$
\begin{aligned}
IDFT\{A(k,l)\} &= \frac{1}{4}MN\Delta\xi\Delta\eta\sum_{m'=-\infty}^{\infty}\sum_{n'=-\infty}^{\infty}\sin c\left(\frac{m'}{2}\right)\\
&\quad \times \sin c\left(\frac{n'}{2}\right)\sin c\left(m - m'\frac{M}{2}\right)\\
&\quad \times \sin c\left(n - n'\frac{N}{2}\right).
\end{aligned}
\tag{3}
$$

$$
\begin{aligned}
IDFT\{U(k,l)\} &= IDFT\{R(k,l)h(k,l)\exp[-j\pi/(\lambda d)\\
&\quad \times (k^2\Delta\xi^2 + l^2\Delta\eta^2)]\}.
\end{aligned}
\tag{4}
$$

where $m=0,1,2,\ldots,M-1$, $n=0,1,2,\ldots,N-1$. m' and n' are the integers. (x,y) is the image plane, $x = m\Delta x$, $y = n\Delta y$. $R(k,l)$ denotes the reference wave for the reconstruction and d is the reconstruction distance. Equation (3) is obtained in terms of the properties of the convolution, the rectangle, and the comb functions as well as their Fourier transforms.

The above results of Eqs. (2)–(4) show that the reconstructed image is characterized by Eq. (4) and modulated by $IDFT\{A(k,l)\}$, i.e., Eq. (3). The latter determines both the amplitude or gray value of every image by $\sin c(m'/2) \sin c(n'/2)$ and the image distribution with the periods of $(M/2,N/2)$ in horizontal and vertical directions, respectively, by $\sin c(m - m'M/2) \sin c(n-n'N/2)$. According to Eq. (3), the image distribution including the zero-order diffraction is illustrated schematically in Fig. 1(a) by taking the in-line geometry as an example, where the shadow areas represent the periodic image distribution. The dc term (white square) is only located at the center of the screen. The reconstructed image at the center actually consists of four quarters that are in the neighboring periods and form a whole image. The zero-order diffractive image is fully superposed with the reconstructed image at the center. According to Eq. (3), the image at the center is of the maximum of gray value and those at the corners are of the minimum of gray value.

To remove the zero-order image, we shift the images with $(M/2,N/2)$ in spatial domain utilizing the space-shifting property of IDFT. This property of the Fourier transform points out that if a function $g(x,y)=IFT\{G(\omega_x,\omega_y)\}$, then

$$g(x+x_0,y+y_0)=IFT\{G(\omega_x,\omega_y)\exp[j\omega(x_0+y_0)]\}, \tag{5}$$

where x_0, y_0 are the shifted distances corresponding to $M/2$ and $N/2$ in horizontal and perpendicular directions, respectively here. Thus, the space-shifting manipulation can be achieved by multiplying a factor $\exp[j\omega(x_0+y_0)]$, the discrete form of which is $(-1)^{k+l}$, with the right side of Eq. (2) before executing IDFT. This manipulation can be expressed as

$$\Gamma(m+M/2,n+N/2)=IDFT\{(-1)^{k+l}A(k,l)\cdot U(k,l)\}. \tag{6}$$

In fact, the space-shifting manipulation is equivalent to the position exchanges between the areas 1 and 3, 2 and 4 due to the periodicity of discrete Fourier transform in a finite range. As a result, the four quarters of the zero-order image are separated and shifted to the corresponding corners accordingly, as they are in different periods, while other images experience only the position exchanges. The above analysis is illustrated by Fig. 1(b).

Although the zero-order diffractive image can be moved away from the center with the space-shifting processing due to its nonperiodicity, the reconstructed image at the center becomes the darkest due to the image exchange. This is obviously insufficient for the image display. To resolve this problem, we combine Fig. 1(a) with Fig. 1(b) using matrix multiplication. With this processing, not only is the dc term eliminated very effectively from the screen but also all periodically distributed images obtain a uniform gray value. This result can be interpreted by the amplitude and distribution modulation factors of the images in Eq. (3). In addition, if we combine the above processing with the intensity-averaging technique [6], the zero-order noises from both object and reference waves can be suppressed more sufficiently, and thus a very clear reconstructed image should be able to be obtained at the center for the in-line digital holography provided that the twin image is eliminated effectively as well.

The experiment is carried out by taking the in-line geometry as an example. The optical setup for recording the holograms is shown in Fig. 2, in which a fundamental mode laser source of model CNI MXL with wavelength $\lambda=532$ nm is used. The hologram is recorded using a complimentary metal-oxide semiconductor (CMOS) with 1280×1024 pixels and 5.2 μm $\times$5.2 μm in pixel sizes. The recording distance, d is 215 mm. O.B. and R.B. are the object and the reference waves, respectively. The reference beam is a plane wave normally incident to the CMOS. BS1 and BS2 are the beam splitters.

The experimental results are shown in Fig. 3, in which Fig. 3(a) is from the Fresnel transformation reconstruction without the use of dc term suppression techniques. The images at the corners show the minimum of gray value. The central image is covered completely by the zero-order image due to the in-line recording of the hologram. In order to exhibit the effect of the space-shifting reconstruction on the dc term removal clearly, the twin image has been pre-eliminated in another way in Fig. 3(a), as the twin image removal has nothing to do with the space-shifting processing and is not the topic that we are concerning about here. The intensity-averaging technique is used in Fig. 3(b) to reduce the dc noises from both object and reference waves, the result from

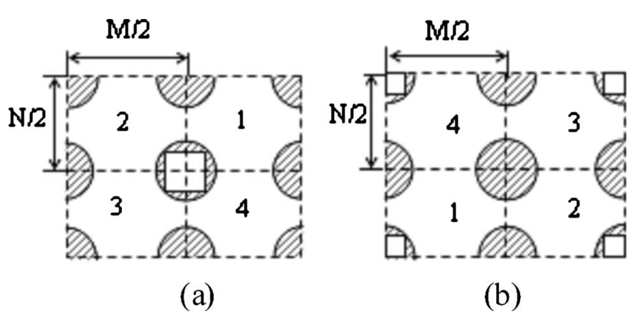

Fig. 1. (a) Periodic image distribution including the zero-order image from the in-line geometry, (b) Position exchanges of the areas 1 and 3, 2 and 4 from the two-dimensional space-shifting manipulation.

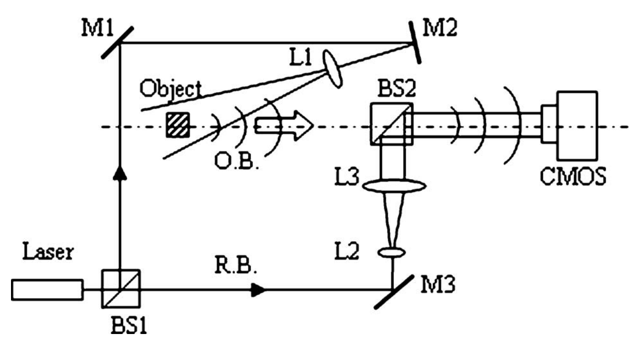

Fig. 2. Experimental setup of recording the in-line digital holograms.

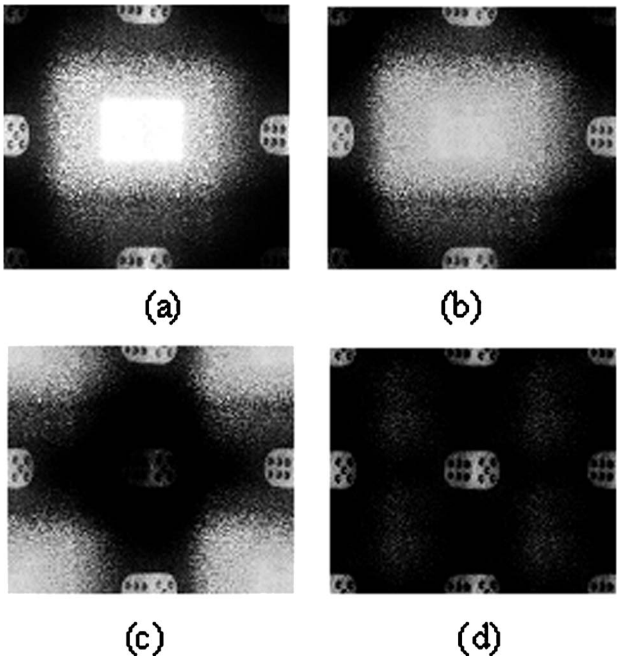

Fig. 3. Experimental results from the in-line digital holography, (a) the hologram reconstruction with the Fresnel transformation without dc term suppression; (b) the use of intensity-averaging technique; (c) the two-dimensional space-shifting manipulation of the images; (d) the final result from the combination of (b) and (c) using matrix multiplication.

which shows that this approach cannot remove the zero-order image completely. The two-dimensional space-shifting manipulation is finished in Fig. 3(c), in which the zero-order image is divided into four quarters and shifted to the corresponding corners and the image at the center becomes the darkest after the image exchange. Finally, the dc term is removed from the screen very effectively by the combination of Figs. 3(b) and 3(c) using matrix multiplication, and all images obtain a uniform gray value as shown in Fig. 3(d). All these results are exactly consistent with our theoretical prediction.

In conclusion, a numerical space-shifting reconstruction approach in digital holography is described here. With this method, not only can the zero-order diffractive image be removed very effectively in the reconstruction, but also all periodically distributed images on the screen obtain a uniform gray value. The experimental results are exactly consistent with the theoretical analysis. Since this approach uses purely numerical processing and so does not need any of additional holograms and specific optical requirements, it can be a really convenient, practical and widely effective way to eliminate the dc term in digital holography.

References

1. U. Schnars and W. Jüptner, *Digital Holography* (Springer, 2005).
2. I. Yamaguchi and T. Zhang, Opt. Lett. **22**, 1268 (1997).
3. J.-P. Liu and T.-C. Poon, Opt. Lett. **34**, 250 (2009).
4. Y. Awatsuji, A. Fujii, T. Kubota, and O. Matoba, Appl. Opt. **45**, 2995 (2006).
5. Y. Awatsuji, M. Sasada, A. Fujii, and T. Kubota, Appl. Opt. **45**, 968 (2006).
6. T. M. Kreis and W. Jüptner, Opt. Eng. **36**, 2357 (1997).
7. C. S. Seelamantula, N. Pavillon, C. Depeursinge, and M. Unser, in *Zero-Order-Free Image Reconstruction in Digital Holographic Microscopy*, IEEE International Symposium on Biomedical Imaging–from Nano to Macro (2009).
8. J. A. H. Ramirez and J. Garcia-Sucerquia, Opt. Commun. **277**, 259 (2007).
9. J. Garcia-Sucerquia, J. A. H. Ramirez, and D. V. Prieto, Proc. SPIE **5622**, 1353 (2004).
10. G.-L. Chen, C.-Y. Lin, M.-K. Kuo, and C.-C. Chang, Opt. Express **15**, 8851 (2007).
11. J. W. Weng, J. G. Zhong, and C. Y. Hu, Opt. Express **16**, 21971 (2008).
12. M. Liebling, T. Blu, and M. Unser, Proc. SPIE **5207**, 553 (2003).
13. C. Liu, Y. Li, X. Cheng, Z. Liu, F. Bo, and J. Zhu, Opt. Eng. **41**, 2434 (2002).
14. E. Cuche, P. Marquet, and C. Depeursinge, Appl. Opt. **39**, 4070 (2000).
15. Y. Zhang, Q. Lu, and B. Ge, Opt. Commun. **240**, 261 (2004).
16. T. M. Kreis, Opt. Eng. **41**, 771 (2002).